

RADIATIVE DECAYS OF THE $\Upsilon(2S)$ RESONANCE

JOACHIM IRION

(REPRESENTING THE CRYSTAL BALL COLLABORATION)¹⁾*Physics Department, Harvard University**Cambridge, Massachusetts 02138*

and

*Stanford Linear Accelerator Center**Stanford University, Stanford, California 94305*

Abstract

The Crystal Ball Detector at DORIS II was used to study radiative decays of the $\Upsilon(2S)$ resonance with more than twice the previously available data. The inclusive photon spectrum of hadronic $\Upsilon(2S)$ decays and the exclusive channel $\Upsilon(2S) \rightarrow \gamma\gamma\Upsilon(1S) \rightarrow \gamma\gamma\ell^+\ell^-$ were analysed. In the inclusive spectrum three significant photon lines at energies of $E_{\gamma_1} = (108.2 \pm 0.7 \pm 4)$ MeV, $E_{\gamma_2} = (127.1 \pm 0.8 \pm 4)$ MeV and $E_{\gamma_3} = (160.0 \pm 2.4 \pm 4)$ MeV with branching fractions of $(6.0 \pm 0.7 \pm 0.9)\%$, $(6.6 \pm 0.8 \pm 1.0)\%$, $(2.6 \pm 0.7 \pm 0.8)\%$ respectively were measured. The lines are consistent with being transitions from the $\Upsilon(2S)$ to the 3P_2 , 3P_1 and 3P_0 states. In addition a line at $E_\gamma \sim 427$ MeV was observed which is interpreted as transitions from the ${}^3P_{2,1}$ states to the $\Upsilon(1S)$.

Invited talk presented at the Rencontre de Moriond: New Particle

Production at High Energy, La Plagne, France, March 4-10, 1984

*Work supported in part by the Department of Energy, contracts DE-AC03-76SF00515 (SLAC) and DE-AC02-76ER03064 (Harvard).

1. Introduction

The Υ resonance family is a system of bound $b\bar{b}$ quarks. Heavy quarkonia systems can be described with the help of potential models^{2]}. The first excited state, the $\Upsilon(2S)$, can decay radiatively through the emission of a photon to the 3P_J states (also called χ_b states). The P states then decay into hadrons or emit a second photon in making the transition to the $\Upsilon(1S)$ ground state. These cascade process are indicated in Fig. 1. The decays are assumed to be electric dipole in nature (E1). Observation of monochromatic photon lines from the $\Upsilon(2S)$ is a signature for these decays. The measurement of the masses of the 3P_J states and the various photon decay rates can be compared with theoretical predictions. The center of gravity of the χ_b lines will test the short range (~ 0.5 fm) behavior of the inter-quark potential. The splitting of the states gives information on the spin-orbit interaction terms and tensor forces of the model. Although the $b\bar{b}$ system is much less relativistic than the charmonium system ($\beta_{b\bar{b}}^2 \sim 0.08$, $\beta_{c\bar{c}}^2 \sim 0.25$) it should also be possible to test for relativistic effects.

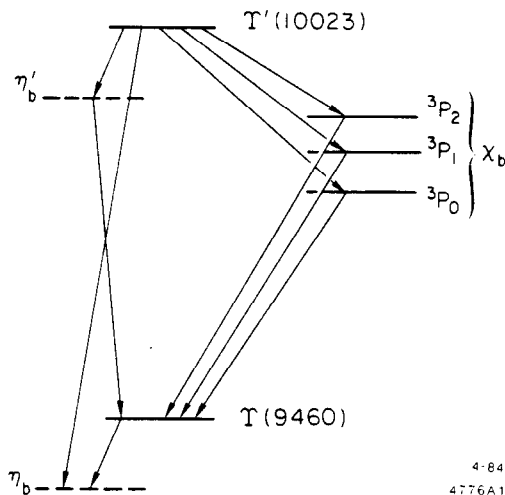


Fig. 1. The level scheme for $b\bar{b}$ bound states below the $\Upsilon(2S)$. The transitions to the χ_b states are electric multipole. Transitions to the η_b states are magnetic multipole and hence suppressed in comparison to the electric transitions.

The Crystal Ball has been taking data on the $\Upsilon(2S)$ resonance at the DORIS storage ring at DESY since Summer 1982 to study these transitions. The results presented in this report are based on $\sim 2 \cdot 10^5$ $\Upsilon(2S)$ decays recorded between Fall 1982 and February 1984.

A schematic drawing of the Crystal Ball as it is installed at DORIS is shown in Fig. 2. A detailed description of the detector can be found elsewhere^{3]}. Therefore, only a brief reiteration of the features relevant to this analysis will be given here. The major component of the detector is a spherical shell of 672 NaI(Tl) crystals, each 16 radiation lengths deep.

They cover 93% of the full solid angle. The energy resolution for electromagnetically interacting particles is

$$\frac{\sigma(E)}{E} = \frac{2.4 - 2.8\%}{E^{1/4}(\text{GeV})}$$

with an angular resolution of 30–50 mrad. Directions of charged particles are measured by three double layers of proportional tube chambers with charge division readout. The energy distribution of charged hadrons peaks around 210 MeV due to non-interacting minimum ionizing particles with a long tail to higher energies caused by nuclear interactions. As there is no magnetic field, momentum measurement of charged particles is not possible.

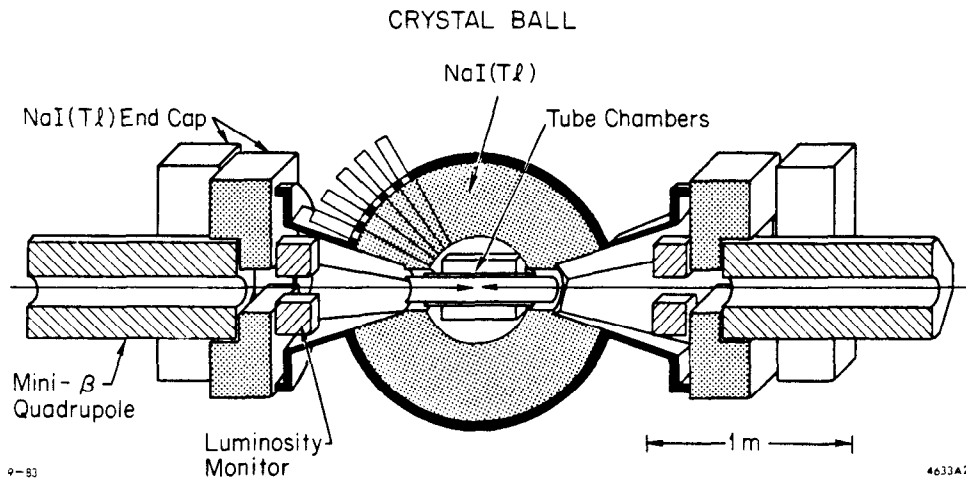
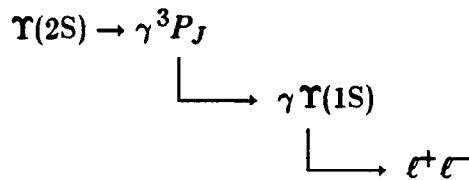


Fig. 2. The Crystal Ball Detector at DORIS II.

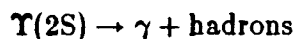
The excellent energy resolution for photons over the large solid angle make the Crystal Ball very well suited to study radiative $\Upsilon(2S)$ decays. This is done in two different ways:

1. Through the exclusive channel



where all decay products are measured ($\ell^+ \ell^-$ is a $\mu^+ \mu^-$ or $e^+ e^-$ pair). The exclusive cascades allow a clean measurement of the event but will have rather limited statistics because of the small $\Upsilon(1S) \rightarrow \ell^+ \ell^-$ branching ratio.

2. Through the inclusive reaction



where one is looking for monochromatic γ lines in the inclusive photon spectrum. The inclusive reaction has a much higher efficiency, but will suffer from high backgrounds. These backgrounds are caused by non-resonance decays, photons from π^0 decays and

charged particles, escaping detection by the tracking chambers. Also, there are photon losses due to overlapping tracks in the high multiplicities of events at these energies.

The complexity of events in the inclusive hadronic sample requires a very involved, time consuming analysis technique. The results of the inclusive analysis presented here correspond to about 3/4 of the total $\Upsilon(2S)$ sample on tape. Because of the rather simple event topology in the exclusive channel, we are able to include the full data sample for this report. The useful luminosities and the number of $\Upsilon(2S)$ decays for both analyses can be found in Table 1.

Table 1
Data Samples used in the Exclusive Cascade Analysis and Inclusive Photon Analysis of $\Upsilon(2S)$ decays.

	$\int \mathcal{L} dt$	Number of $\Upsilon(2S)$ decays
Exclusive Analysis	$\sim 64.5 \text{ pb}^{-1}$	$(200 \pm 15) \cdot 10^3$
Inclusive Analysis	$\sim 49.3 \text{ pb}^{-1}$	$(151 \pm 10) \cdot 10^3$

2. Exclusive Cascade Analysis

First, we shall focus on the exclusive analysis. The four stages of the event selection for this process are outlined below:

1. As a first step in the analysis events with the desired topology are selected: a total number of four particles in the ball within $|\cos\theta_z| < 0.85$, where θ_z is the angle of the particle with respect to the beam. Two of the four particles, the lepton candidates, have to be emitted nearly back-to-back ($\Theta_{ij} > 160^\circ$, where Θ_{ij} is the angle between two particles).
2. Each of the particles forming the back-to-back pair must satisfy the condition $E > 3000$ MeV (for electron candidates) or deposit an energy between $160 \text{ MeV} < E < 300 \text{ MeV}$ in a small number of crystals (≤ 4). The latter is typical for muons. For events surviving these cuts we plot in Fig. 3 the mass recoiling against the two photon candidates. The distribution shows a very clean peak around the $\Upsilon(1S)$ mass. It is a good indication that indeed we see photon transitions from the $\Upsilon(2S)$ to the $\Upsilon(1S)$ ground state.
3. The background in Fig. 3 can be reduced by requiring that the charged lepton pair gets recognized as such by the chambers and that none of the tracks may overlap with each other. This is to ensure a clean measurement of the photon energies.
4. The surviving events are fitted to the hypothesis $e^+e^- \rightarrow \gamma\gamma\ell^+\ell^-$. For the electron channel this is a four constraint fit (4C), since the four-momenta of all final state particles are measured. In the $\mu^+\mu^-$ channel only the muon directions but not their energies are measured, resulting in a two constraint fit (2C). The fit does not use a constraint on the $\Upsilon(1S)$ mass for the $\ell^+\ell^-$ pair. Events are rejected if the confidence level of the fit is less than 10%.

The information obtained so far is displayed in Fig. 4(a), where the energy of the lowest energy photon ($E_{\gamma,low}$) is plotted against the observed $\Upsilon(2S) - \Upsilon(1S)$ mass difference,

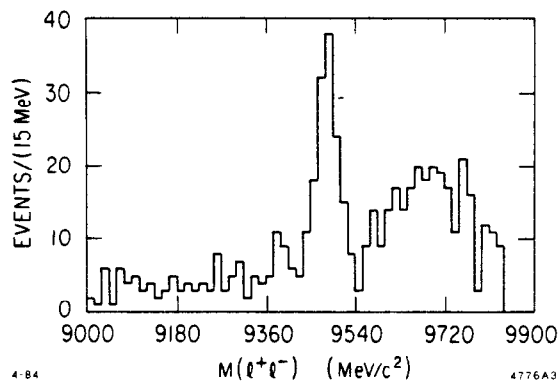


Fig. 3. A plot of the recoil mass ($M_{\ell^+\ell^-}$) in the exclusive channel $\Upsilon(2S) \rightarrow \gamma\gamma \ell^+\ell^-$ after selecting events of this topology.

defined by $\Delta M = M(\Upsilon(2S)) - M(\ell^+\ell^-)$, where $M(\ell^+\ell^-)$ is the mass recoiling against the two photons. A clustering of events at a value consistent with the $\Upsilon(2S) - \Upsilon(1S)$ mass difference* and at two distinct values of $E_{\gamma,low}$ are prominent.

To obtain the energy spectrum of the low energy photons a cut around the $\Upsilon(2S) - \Upsilon(1S)$ mass difference of $500 \text{ MeV}/c^2 < \Delta M < 590 \text{ MeV}/c^2$ (a $\pm 3\sigma$ cut) is applied [see Fig. 4(b)]. The resulting photon spectrum is shown in Fig. 5. The distribution now shows two clean, separated peaks. A fit to the distribution with two Gaussians with variable means, widths and amplitudes on a constant background determines the energies of the lines to be $E_{\gamma 1} = (101.2 \pm 1.3) \text{ MeV}$ and $E_{\gamma 2} = (125.2 \pm 1.3) \text{ MeV}$. The fitted widths of the lines are consistent with our resolution. We estimate the systematic error on the energy measurement to be $\pm 4\%$ for both lines. There are 34 $\mu^+\mu^-$ decays and 33 e^+e^- decays surviving all the cuts. In this sample there is no indication of a third line. This is not surprising as theory indicates a very small branching ratio for one of the P states (3P_0) to decay to the ground state by photon emission⁴].

At the time of writing this report the systematic errors in the efficiency calculations are still large. Therefore, we cannot yet add additional information on the branching ratios in the exclusive channel as previously published⁵].

3. Inclusive Photon Analysis

In this section we examine the inclusive photon spectrum in hadronic decays of the $\Upsilon(2S)$, where the 3P_J states are detected through the presence of monochromatic photon lines.

The analysis described below differs in some points from an earlier study the Crystal Ball performed with the data available in Summer 1983⁶]. Compared to Summer 1983 more than twice the previous data are now available and improved selection criteria to resolve the primary photon lines can be applied. The analysis proceeds as follows:

* We observe a small ($\sim 4\%$) energy shift in the exclusive events towards lower energies. This is also seen in the reaction $\Upsilon(2S) \rightarrow \pi^0\pi^0\Upsilon(1S)$, see Ref. 6. The cuts used are adjusted for this shift.

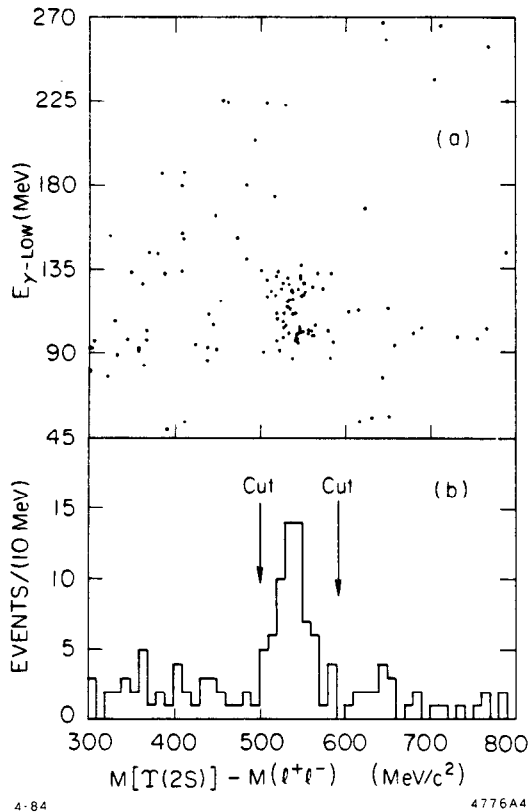


Fig. 4. (a) Scatter plot of the energy of the low energy photon in the reaction $\Upsilon(2S) \rightarrow \gamma\gamma\ell^+\ell^-$ vs. the mass difference $M(\Upsilon(2S)) - M(\ell^+\ell^-)$. $M(\ell^+\ell^-)$ is calculated as the mass recoiling against the $\gamma\gamma$ system, and (b) Projection of Fig. 4(a) on the mass difference axis. A cut was made at 545 ± 45 MeV to select cascade events.

From all the recorded triggers hadronic events are selected by removing backgrounds from beam-gas interactions, QED events and cosmic rays. The efficiency of the selection is found to be $\epsilon_h = (0.85 \pm 0.05)\%$ using Monte Carlo calculations. Details on the selection criteria and efficiency calculation of the hadron selection can be found in Ref. 7. The resulting sample of hadronic events contains contributions from resonance and continuum decays in about a one to one ratio.

The cuts to identify photons in these events are designed to remove charged particles, photons forming π^0 s and photons with showers contaminated by energy depositions from nearby particles:

1. A photon track must be within a solid angle of $|\cos\theta_z| < 0.75$ (θ_z is the angle of the photon direction with respect to the beam). This is the acceptance covered by all three tube chambers. The track must be neutral i.e., it may not be correlated with hits in the tracking chambers. The energy spectrum of tracks satisfying the above requirements is shown in Fig. 6(a) on a logarithmic scale. Structures in the range of 100 to 170 MeV and at about 430 MeV are visible. The residual peak around 210 MeV is a manifestation of misidentified charged particles. The broad shoulder on the low energy side at about 30 to 40 MeV is due to large fluctuations in the shower development of electrons and photons

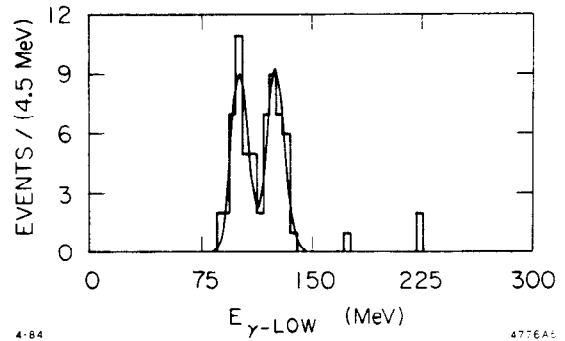


Fig. 5. Energy distribution of the low energy photon from the final cascade sample $[\Upsilon(2S) \rightarrow \gamma\gamma\ell^+\ell^-]$. The curve is a fit to the data as described in the text.

or remnants from nuclear interactions causing additional energy deposits away from the original impact point.

2. To obtain the best energy measurement for the photon candidates their energy clusters must be well separated from other tracks.
3. To further reduce the still appreciable background from charged particles in Fig. 6(a) the more restrictive requirement that not even one of the individual crystals associated with the photon shower may be correlated with a hit in the chambers is applied.
4. The lateral energy distribution in the crystals has to be consistent with the typical pattern of a single electromagnetic shower.
5. Photon pairs which reconstruct to the π^0 mass are removed.

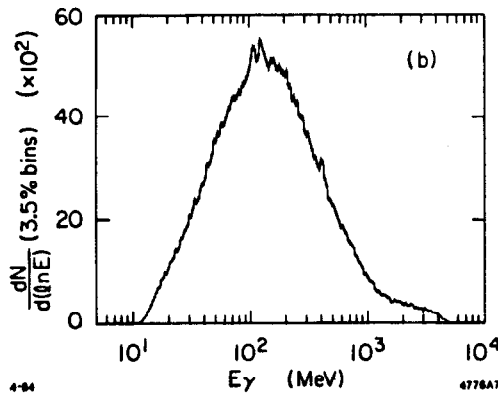
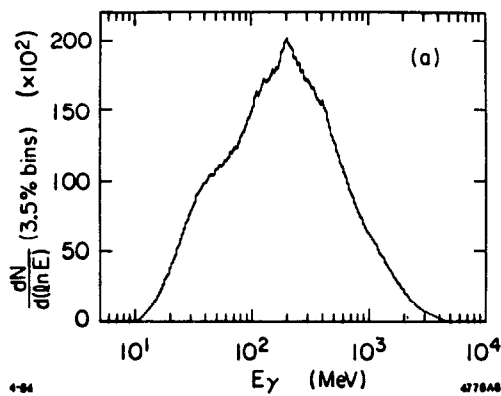


Fig. 6. Inclusive photon spectra from hadronic decays of the $\Upsilon(2S)$: (a) All neutral tracks in the solid angle covered by the chambers, and (b) After applying all the photon selection criteria described in the text.

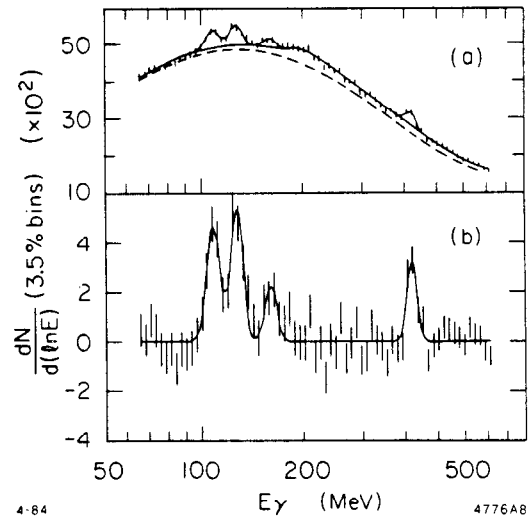


Fig. 7. (a) A fit to the photon spectrum of Fig. 6(b) with a model for cascade transitions from the $\Upsilon(2S)$. Details of the model are explained in the text, and (b) The fit of Fig. 7(a) after subtracting the polynomial background and the background due to charged particles.

Figure 6(b) shows the inclusive photon spectrum after all the above cuts. Three peaks in the region of 100 to 170 MeV and another bump around 430 MeV are clearly visible. Note that the enhancement at around 30 to 40 MeV has disappeared and that the charged particle “punch through” is greatly reduced, though still visible as a shoulder around 210 MeV.

To obtain the number of photons in the observed peaks we fit part of the spectrum between $E_\gamma \sim 65$ MeV and $E_\gamma \sim 720$ MeV with the following model of cascade transitions from the $\Upsilon(2S)$:

1. Three Gaussian distributions with fixed widths given by our resolution to describe the region between 100 MeV and 170 MeV.
2. Two Gaussian distributions, each convoluted with an appropriate Doppler box, to describe the daughter lines (from the 3P_2 and 3P_1 states) at about 430 MeV. Their energies were calculated from the primary lines and the known masses of $\Upsilon(2S)$ and $\Upsilon(1S)$ (see Ref. 8).
3. A smooth fifth order polynomial background.
4. A charged particle spectrum with variable amplitude. This spectrum was obtained by taking genuine charged particles as defined by the tracking chambers and imposing the same cuts on them as used for the photon selection.

Only two daughter lines were taken as the 3P_0 state is expected to have only a small branching ratio to decay radiatively to the $\Upsilon(1S)$ ground state. This is also indicated by our study of the exclusive channel. The resulting fit, displayed in Fig. 7, has an good χ^2/df of 0.9. The dashed line in Fig. 7(a) represents the smooth polynomial background. The amount of charged particle background is given by the difference of the solid line (excluding the Gaussians) and the dashed line. In Fig. 7(b) this background has been subtracted.

We observe three significant low energy lines at energies of $E_{\gamma 1} = (108.2 \pm 0.7)$ MeV, $E_{\gamma 2} = (127.1 \pm 0.8)$ MeV, $E_{\gamma 3} = (160.0 \pm 2.4)$ MeV and a peak associated with the daughter lines at an average energy* of $\langle E_\gamma \rangle = 427$ MeV (see also Table 2). The systematic error on the energy measurement of the lines is again $\pm 4\%$.

In order to calculate branching ratios for the observed transitions, the photon detection efficiencies need to be determined in the range from 90 MeV to 500 MeV. The procedure of the calculation is detailed in Ref. 9. For the final spectrum [Fig. 6(b)] the efficiency is found to be $(21.0 \pm 0.7 \pm 2)\%$ and nearly constant over the range of interest. Here, the first error is statistical and the second error reflects the systematic uncertainties.

* The daughter lines are too closely spaced to be resolved by our detector.

Table 2

Photon lines observed from inclusive $\Upsilon(2S)$ decays. The statistical significances in standard deviations (s.d.) have been evaluated independently of the systematic errors in the branching ratios.

	Photon energy (MeV)	Significance (s.d.)	Overall efficiency (%)	Branching ratio (%)
This experiment ^{a)}	$108.2 \pm 0.7 \pm 4$	8.6	16.6 ± 2.5	$6.0 \pm 0.7 \pm 0.9$
	$127.1 \pm 0.8 \pm 4$	8.3	16.6 ± 2.5	$6.6 \pm 0.8 \pm 1.0$
	$160.0 \pm 2.4 \pm 4$	3.9	16.6 ± 5.0	$2.6 \pm 0.7 \pm 0.8$
	<427>	5.6	17.4 ± 2.6	$2.9 \pm 0.5 \pm 0.4$
CUSB ¹¹⁾	$108.2 \pm 0.3 \pm 2$	4.4	13	6.1 ± 1.4
	$128.1 \pm 0.4 \pm 3$	4.2	13	5.9 ± 1.4
	$149.4 \pm 0.7 \pm 5$	2.5	13	3.5 ± 1.4
	$427.0 \pm 1.0 \pm 8$	4.0	13	4.0 ± 1.0
CLEO ^{10) b)}	$109.5 \pm 0.7 \pm 1$	5.7	2.5	$10.2 \pm 1.8 \pm 2.1$
	$129.0 \pm 0.8 \pm 1$	4.7	3.2	$8.0 \pm 1.7 \pm 1.6$
	$158.0 \pm 7.0 \pm 1$	1.9	3.6	$4.4 \pm 2.3 \pm 0.9$

^{a)} Isotropic photon distributions assumed. A $1 + \cos^2 \theta$ distribution for the line at 160 MeV (χ_0 hypothesis) would raise this branching ratio by $\sim 10\%$. The error in the efficiency includes an estimate of the systematics.

^{b)} The line at 158 MeV is not clearly implied by the data.

4. Results

The branching ratios (BR) for the observed signals in the inclusive analysis have been calculated according to

$$BR = \frac{N_\gamma}{N_{\Upsilon(2S)}} \cdot \frac{1}{\epsilon_{tot}}$$

where

N_γ is the number of photons in a given line determined by the fit,

$N_{\Upsilon(2S)}$ is the total number of $\Upsilon(2S)$ resonance decays,

ϵ_{tot} is the total detection efficiency for a photon of a given E_γ . Included in this efficiency is the photon efficiency described above and the efficiency to detect the final state. Also taken into account are losses due to photon conversions in the beam pipe and the chambers. Note, that isotropic photon directions are assumed.

The energies of the observed lines, their significance (in standard deviations), the total detection efficiencies and resulting branching ratios are listed in Table 2. The relative strengths of the two lines contributing to the line at about 427 MeV are poorly determined by the fit. Therefore the branching ratio for this line may be interpreted as the sum of the individual branching ratio products $BR(\Upsilon(2S) \rightarrow \gamma^3P_2) \cdot BR(^3P_2 \rightarrow \gamma\Upsilon(1S))$ and $BR(\Upsilon(2S) \rightarrow \gamma^3P_1) \cdot BR(^3P_1 \rightarrow \gamma\Upsilon(1S))$. Also listed in Table 2 are the values obtained by the CLEO^{10]} and CUSB^{11]} collaborations. In Table 3 we compare our measurements with some theoretical predictions^{12]-17]}. Here we assume that the three low energetic photon lines come from the decays $\Upsilon(2S) \rightarrow \gamma^3P_{2,1,0}$ in order of increasing energy to calculate the corresponding masses. With the present experimental errors there is reasonable agreement between our results and the corresponding quantities as calculated in a variety of potential models. At present, however, it is not possible to definitely confirm or rule out certain calculations. The observed line splittings seem to agree most with the model of Gupta *et al.*^{14]}.

5. Conclusions

In the inclusive photon spectrum from hadronic decays of the $\Upsilon(2S)$ we observe three well separated photon lines presumably corresponding to the transitions $\Upsilon(2S) \rightarrow \gamma^3P_2, ^3P_1, ^3P_0$ and another photon peak consistent with the (unresolved) transitions $^3P_2, ^3P_1 \rightarrow \gamma\Upsilon(1S)$. The statistical significance of the weakest line ($\Upsilon(2S) \rightarrow \gamma^3P_0$) is 3.9 standard deviations. From the energies of the first three lines we give a complete measurement of the fine splitting

Table 3

Comparison of experimental results from the Inclusive Photon Analysis with theoretical predictions.

	$M_{COG}^a)$ (MeV/c ²)	$\Delta M_2^b)$ (MeV/c ²)	$\Delta M_1^b)$ (MeV/c ²)	$\Delta M_0^b)$ (MeV/c ²)	$\frac{\Gamma(^3P_J)}{(2J+1)E_J^3} \cdot \frac{3E_1^3}{\Gamma(^3P_1)}$
This experiment ^{c)}	9902.1 ± 2.7	12.2 ± 3.2	-6.9 ± 3.8	-40.3 ± 5.0	$J = 2 : 0.9 \pm 0.3$ $J = 0 : 0.6 \pm 0.3$
Khare ¹²⁾	9871.0	8.0	-4.0	-28.0	
Eichten, Feinberg ¹³⁾	9924.7	14.3	-11.7	-36.7	
Gupta, et al. ¹⁴⁾	9899.7	10.3	-6.7	-32.7	
Buchmüller ^{d) 15)}	9888.4	9.6	-6.4	-28.4	$J = 2 : 1.03$ $J = 1 : 1.03$
Moxhay, Rosner ¹⁶⁾	9906.2	7.8	-3.2	-29.2	$J = 2 : 1.05$ $J = 1 : 0.88$
McClary, Byers ¹⁷⁾	9922.8	15.2	-6.8	-55.8	$J = 2 : 1.13$ $J = 1 : 0.76$

a) $M_{COG} = \Sigma(2J + 1)M(^3P_J)/9$.

b) $\Delta M_J = M(^3P_J) - M_{COG}$.

c) Errors include statistical and systematic uncertainties.

d) Masses scaled by 27 MeV for correct $\Upsilon(1S)$ mass.

of the 3P_J states. Additional evidence for the radiative decays of the $\Upsilon(2S)$ comes from our study of the exclusive channels, where we observe the transitions $\Upsilon(2S) \rightarrow \gamma_1 ^3P_2 \rightarrow \gamma_1(\gamma_2 \Upsilon(1S))$ and $\Upsilon(2S) \rightarrow \gamma_3 ^3P_1 \rightarrow \gamma_3(\gamma_4 \Upsilon(1S))$. Our results are compared with the predictions of various potential model calculations.

REFERENCES

1. C. Edwards, C. Peck, F. Porter, P. Ratoff (California Institute of Technology, Pasadena, USA); I. Brock, A. Engler, B. Kraemer, D. Marlow, F. Messing, D. Prindle, B. Renger, C. Rippich (Carnegie-Mellon University, Pittsburgh, USA); Z. Jakubowski, B. Niczyporuk, G. Nowak, T. Skwarnicki (Cracow Institute of Nuclear Physics, Cracow, Poland); J. K. Bienlein, S. Cooper, B. Gomez, T. Kloiber, W. Koch, M. Schmitz, H.-J. Trost, P. Zschorsch (Deutsches Elektronen Synchrotron DESY, Hamburg, Germany); D. Antreasyan, J. Irion, K. Strauch, D. Williams (Harvard University, Cambridge, USA); D. Besset, R. Cabenda, M. Cavalli-Sforza, R. Cowan, D. Coyne, C. Newman-Holmes (Princeton University, Princeton, USA); E. Bloom, R. Chestnut, R. Clare, J. Gaiser, G. Godfrey, S. Leffler, W. Lockman, S. Lowe, K. Wacker (Stanford Linear Accelerator Center, Stanford University, Stanford, USA); D. Gelpman, R. Hofstadter, I. Kirkbride, R. Lee, A. Litke, T. Matsui, B. Pollock, J. Tompkins (Stanford University, Department of Physics and HEPL, Stanford, USA.) G. Folger, B. Lurz, U. Volland, H. Wegener (Universität Erlangen-Nürnberg, Erlangen, Germany); A. Cartacci, G. Conforto, D. de Giudibus, B. Monteleoni, P. G. Pelfer (INFN and University of Firenze, Italy); A. Fridman, F. Heimlich, R. Lekebusch, P. Lezoch, W. Maschman, R. Nernst, A. Schwarz, D. Sievers, U. Strobusch (Universität Hamburg, I. Institut für Experimentalphysik, Hamburg, Germany); A. König, J. Schotanus, R. T. Van de Walle, W. Walk, W. Metzger (University of Nijmegen, The Netherlands); S. Keh, H. Kilian, K. Königsmann, M. Scheer, P. Schmitt (Universität Würzburg, Germany); D. Aschman (University of Cape Town, South Africa).
2. For various potential models see refs. 12)–17)
3. M. Oreglia *et al.*, Phys. Rev. D25, 2259 (1983) M. Oreglia, Ph.D. Thesis, Stanford University, SLAC-PUB-236 (1980); J. Gaiser, Ph.D. Thesis, Stanford University, SLAC-PUB-255 (1982)
4. Y. P. Kuang and T.M. Yan, Phys. Rev. D24, 2874 (1981)
5. F. Pauss *et al.*, Phys. Lett. 130B, 439 (1983)
6. J. Gaiser, "Results from the Crystal Ball at DORIS II", Proc. of the 11th SLAC Summer Institute on Particle Physics Stanford, July 18-29, 1983, SLAC Report No. 267 (1984).
7. C. Edwards *et al.*, SLAC-PUB-3030 (1983); H.-J. Trost, private communication.
8. D. P. Barber *et al.*, Phys. Lett. 135B, 498 (1984); A. S. Artamonov *et al.*, Phys. Lett. 137B, 272 (1984).
9. J. Gaiser, see Ref. 3)
10. P. Haas *et al.*, Phys. Rev. Lett. 52, 799 (1984)
11. C. Klopfenstein *et al.*, Phys. Rev. Lett. 51, 160 (1983)
12. A. Khare, Phys. Lett., 98B, 385 (1981)
13. E. Eichten and F. Feinberg, Phys. Rev. D23, 2724 (1981)
14. S. N. Gupta *et al.*, Phys. Rev. D26, 3305 (1982)
15. W. Buchmüller, Proc. of the 2nd Moriond Workshop on New Flavours, Les Arcs, Savoie, France, Jan. 24-30, 1982, Editions Frontières, France (1982).
16. P. Moxhay and J. L. Rosner, Phys. Rev. D28, 1132 (1983)
17. R. McClary and N. Byers, Phys. Rev. D28, 1692 (1983)